NeuroImage: Clinical 22 (2019) 101682

Contents lists available at ScienceDirect

NeuroImage: Clinical

journal homepage: www.elsevier.com/locate/ynicl

Structural covariance in subcortical stroke patients measured by automated MRI-based volumetry

Caihong Wang[a,1], Lei Zhao[b,1], Yishan Luo[b], Jingchun Liu[c], Peifang Miao[a], Sen Wei[d], Lin Shi[b,e,*], Jingliang Cheng[a,**]

[a] Department of MRI, The First Affiliated Hospital of Zhengzhou University, Zhengzhou, China
[b] BrainNow Research Institute, Shenzhen, Guangdong Province, China
[c] Department of Radiology, Tianjin Key Laboratory of Functional Imaging, Tianjin Medical University General Hospital, Tianjin, China
[d] Department of Neurology, The First Affiliated Hospital of Zhengzhou University, Zhengzhou, China
[e] Department of Imaging and Interventional Radiology, The Chinese University of Hong Kong, Shatin, Hong Kong

ARTICLE INFO

Keywords:
Brain segmentation
Brain volumetric changes
MRI imaging
Stroke
Structural covariance
Lesion-side effect

ABSTRACT

A network-level investigation of the volumetric changes of subcortical stroke patients is still lacking. Here, we explored the alterations of structural covariance caused by subcortical stroke with automated brain volumetry. T1-weighed brain MRI scans were obtained from 63 normal controls (NC), 46 stroke patients with infarct in left internal capsule (CI_L), 33 stroke patients with infarct in right internal capsule (CI_R). We performed automatic anatomical segmentation of the T1-weighted brain images with AccuBrain. Volumetric structural covariance analyses were first performed within the basal ganglia structures that were both identified by voxel-based morphometry with AAL atlas and AccuBrain. Subsequently, we additionally included the infratentorial regions that were particularly quantified by AccuBrain for the structural covariance analyses and investigated the alterations of anatomical connections within these subcortical regions in CI_L and CI_R compared with NC. The association between the regional brain volumetry and motor function was also evaluated in stroke groups. There were significant and extensive volumetric differences in stroke patients. These significant regions were generally symmetric for CI_L and CI_R group depending on the side of stroke, involving both regions close to lesions and remote regions. The structural covariance analyses revealed the synergy volume alteration in subcortical regions both in CI_L and CI_R group. In addition, the alterations of volumetric structural covariance were more extensive in CI_L group than CI_R group. Moreover, we found that the subcortical regions with atrophy contributed to the deficits of motor function in CI_R group but not CI_L group, indicating a lesion-side effect of brain volumetric changes after stroke. These findings indicated that the chronic subcortical stroke patients have extensive disordered anatomical connections involving the whole-brain level network, and the connections patterns depend on the lesion-side.

1. Introduction

The subcortical infarction generally causes impairment in the motor pathway, and a multitude of neuroimaging studies have demonstrated that subcortical stroke-induced alterations may present beyond the motor system and manifest as the involvement of multiple functional systems. For instance, the functional magnetic resonance imaging (MRI) demonstrated altered activation within the motor network and in other functional network and their interaction between the functional networks after subcortical stroke (Wang et al., 2014). The brain morphometric studies based on structural MRI revealed multiregional gray matter volume changes in subcortical stroke patients, not only in brain regions adjacent to stroke lesions but also in the areas remote to lesions during recovery (Anderson et al., 2002; Zhang et al., 2014; Diao et al., 2017a,b). However, the existing morphometric studies mostly focus on cortical gray matter structural changes, and the structural alterations of subcortical regions and infratentorial regions are rarely studied.

In addition, it has been realized that communities of brain regions co-vary in their morphological properties (such as gray matter volume,

* Correspondence to: L. Shi, BrainNow Research Institute, Shenzhen, Guangdong Province, China.
** Corresponding author.
E-mail addresses: shilin@cuhk.edu.hk (L. Shi), fccchengjl@zzu.edu.com (J. Cheng).
[1] These authors contributed equally to the work.

https://doi.org/10.1016/j.nicl.2019.101682
Received 12 November 2018; Received in revised form 27 December 2018; Accepted 20 January 2019
Available online 22 January 2019

surface area and cortical thickness (Mechelli et al., 2005; Bernhardt et al., 2008; Sanabria-Diaz et al., 2010)), which is called structural covariance (Alexander-Bloch et al., 2013b; Chong et al., 2017). The structural covariance primarily reflects inter-regional coordination in the development process or synchronous effects on the connected regions (DuPre and Spreng, 2017), and such networks of structural covariance are associated with behavioral and cognitive abilities (Alexander-Bloch et al., 2013a). Although the alterations of structural covariance have been associated with aging (Hafkemeijer et al., 2014), psychiatric disorders (Liu et al., 2016; Cauda et al., 2018; Jiang et al., 2018; Liu et al., 2018) and many neurodegenerative diseases (Seeley et al., 2009; Nestor et al., 2017; Lee et al., 2018) in the previous studies, the relevant investigation into stroke is still insufficient, especially for subcortical stroke patients.

Benjamin and his colleagues (Benjamin et al., 2014) investigated the structural covariance of whole-brain level gray matter and white matter densities with the average gray matter density of the lesioned subcortical region on a voxel-wise basis, but the lesion distribution was rather dispersed throughout the subcortical gray matter and white matter, making their results not generalizable to a specific subcortical stroke cohort. Another two studies (Fan et al., 2013; Abela et al., 2015) associated the longitudinal alterations of structural covariance with motor recovery of ischemic stroke, but they also suffered from the dispersed lesion distribution and their results of structural covariance could not be generalized to a cohort with a centralized lesion distribution within a specific region. Moreover, all these studies used the imaging feature extracted from normalized gray matter (GM) density map in voxel-based morphometry (VBM) analyses (Seeley et al., 2009). While this voxel-based method helps achieving high spatial resolution of the structural covariance, it cannot measure the cumulative alteration of the volumetric correlations between anatomical subcortical structures. Although the normalized GM density maps could also be projected to public brain atlases (e.g. automated anatomical labeling (AAL) atlas) with modulation to measure the GM volume of a specific anatomic structure as in other studies (Alexander-Bloch et al., 2013b; Kim et al., 2015), this method has been reported with lower accuracy compared with anatomic segmentation tools (e.g. FreeSurfer) in subcortical structures (Naess-Schmidt et al., 2016).

In such background, we aimed to investigate the brain volumetric changes and the alterations of structural covariance in a cohort of subcortical stroke patients with infarction centralized to internal capsular regions. A multi-atlas-based anatomical segmentation tool *AccuBrain*, which has demonstrated its best accuracy of segmentation in subcortical structures such as hippocampus (Abrigo et al., 2018) among the existing segmentation tools, was used for the quantification of brain volumetry and the volumetric structural covariance. In this study, we focused on the analyses of structural covariance within the subcortical (close to lesions) and infratentorial (remote to lesions) regions that involve motor pathway. To compare with the general VBM-based structural covariance method, we also performed a sub-analysis of volumetric structural covariance within the basal ganglia structures that were both available for quantification in AccuBrain and VBM (with AAL atlas).

Furthermore, a multitude of neuroimaging studies have shown that the cerebral hemispheric asymmetry (Chiu and Damasio, 1980; LeMay, 1986; Corballis, 2014) may result in different structural reorganization following stroke in the homologous region of the left and right hemispheres, and the lesion-side effect has been found in gray matter volume changes in subcortical stroke patients (Diao et al., 2017a, 2017b). In this case, the analyses in our study were further refined according to the side of the lesions, as it would be also interesting to investigate whether patients with lesions in the left and right hemispheres exhibit similar or different patterns in brain structural damage and volumetric structural covariance. Also, the associations between the quantified brain regions with atrophy and motor function after stroke were investigated to see if the regions that triggered most changes of anatomic connections in subcortical stroke would consistently present significant impact on motor function.

2. Method

2.1. Subjects

MRI data were collected by two scanners from two hospitals (The First Affiliated Hospital of Zhengzhou University and Tianjin Medical University General Hospital). The experimental protocol was approved by the local Medical Research Ethics Committee, and written informed consent was obtained from all participants or patient's legal guardian. All the patients were first-onset ischemic stroke patients and showed motor deficits in both the upper and lower extremities at stroke onset. In addition, the amount of time after stroke onset was > 6 months to ensure that the patients were at a stable chronic stage. Regarding the lesion location, it was restricted to the internal capsule and/or surrounding areas (involving basal ganglia, thalamus, coronal radiata) with only a single lesion of ischemic infarct. Furthermore, we also excluded the subjects with recurrent stroke (defined based on both clinical history and MRI evaluation), those with lacunes or microbleeds (based on T1-, T2 FLAIR-weighted images and eSWAN), and those with severe white matter hyperintensity (manifesting as a Fazekas et al. (1987) scale score > 1). Finally, 79 chronic subcortical stroke patients (46 with infarct in the left internal capsular (CI_L) and 33 with infarct in the right internal capsular (CI_R)) and 63 normal controls (NC) were included in this study. All these subjects were right-handed. Moreover, to investigate the effect of lesion side, stroke patients with the left and right lesions were analyzed separately. Fugl-Meyer assessment (FMA) was used to assess motor function of stroke patients.

Lesion location of each stroke patient was determined by an experienced neuroradiologist on 3D T1-weighted MRI images. Firstly, the T1-weighted images was spatially normalized to MNI space. Afterwards, we manually delineated the lesions on the normalized T1-weighted MRI images slice by slice using the software MRIcron (http://www.mccauslandcenter.sc.edu/mricro/mricron/). Accordingly, a lesion mask was generated for each subject. Finally, the lesion masks of all stroke patients were overlapped and overlaid on an MNI template to create the lesion probability map as depicted in Fig. 1.

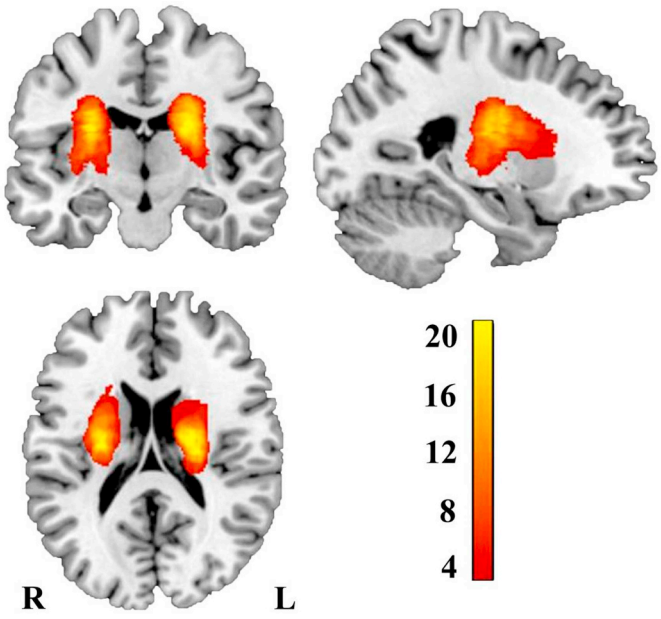

Fig. 1. Lesion incidence map of patients with stroke. Color represents lesion incidence frequency. (For interpretation of the references to color in this figure legend, the reader is referred to the web version of this article.)

2.2. Image acquisition

Two 3.0-Tesla MR imaging system from two Discovery MR 750 scanner (GE Medical Systems) was used for image acquisition. Three-dimensional sagittal T1-weighted images were acquired using a magnetization prepared rapid acquisition gradient echo sequence with following parameters: repetition time (TR) = 8.14 ms, echo time (TE) = 3.17 ms, flip angle (FA) = 12°, inversion time (TI) = 450 ms, matrix = 256 × 256, FOV = 256 × 256 mm^2, number of slices = 188, slice thickness = 1.0 mm, no gap, spatial resolution = 1 × 1 × 1 mm^3 and acquisition time = 4min10s. T2 FLAIR sequences were acquired at the axial plane with TR = 8500 ms, TE = 157.73 ms, FA = 111°, TI = 2100 ms, matrix = 256 × 256, number of slices = 20, and slice thickness = 5.0 mm and acquisition time = 2min52s. eSWAN sequences were acquired at the axial plane with TR = 35.7 ms, TE = 3.8 ms, FA = 20°, matrix = 320 × 256, FOV = 220 × 220 mm^2, number of slices = 80, slice thickness = 2.0 mm and acquisition time = 3min52s.

2.3. Image processing

The analyses of image processing were performed blind. The T1-weighted MRI scans were automatically segmented with *AccuBrain*, which enables segmentation and quantification of cortical, subcortical and infratentorial structures based on statistical prior anatomical knowledge by experienced radiologists with 5 years' experience (Abrigo et al., 2018). In detail, this segmentation tool utilized a multi-atlas-based segmentation method (Nestor et al., 2013), where the atlas pool was derived from many brain MR images acquired from different scanners, together with the prior anatomical information of radiologists in the brain structures to be delineated. A number of atlases were screened from this atlas pool based on the similarity between the atlas image and the individual image, and then nonrigid image registration was performed to project the selected atlases to individual space. The final segmentation labels of a subject were realized by label fusion that fused the labels from the screened atlases in individual space. In a recent validation study based on a standard dataset from the from the European Alzheimer's Disease Consortium - Alzheimer's Disease Neuroimaging Initiative Harmonized Protocol (EADC-ADNI HarP) where manual hippocampal segmentation reference was available, AccuBrain achieved the best performance among the existing automatic brain segmentation tools (Abrigo et al., 2018). Here, we selected all the typical subcortical brain regions that were available for segmentation in *AccuBrain*, including basal ganglia structures that were close to the lesioned internal capsular (amygdala, hippocampus, thalamus, caudate, putamen, pallidum, accumbens area, and ventral diencephalon (DC)), and remote structures (midbrain, pons, medulla oblongata, and superior cerebellar peduncle (SCP)). Also, we measured brain parenchyma and lateral ventricle with AccuBrain as they reflect the degree of brain atrophy in a global scale. The volumes of these subcortical structures were divided by the intracranial volume (ICV) for each subject as a normalization process (regional brain volume/ICV × 100%) for the subsequent analyses. Here, the ICV was defined as volume within the cranium, including the brain, meninges and CSF (Whitwell et al., 2001).

To validate the use of brain volumes obtained from AccuBrain for the subsequent structural covariance analyses, we also performed tissue segmentation with the Computational Anatomy Toolbox (CAT12) via the current version of Statistical Parametric Mapping software (SPM12) (http://www.neuro.uni-jena.de/cat/). SPM is a widely-used tool for VBM analysis that helps to identify the brain volumetric changes, which is mostly used for structural covariance analysis. Within the pipeline of VBM, the brain images were first segmented in individual space into different tissue maps (such as GM, white matter and cerebrospinal fluid (CSF)) and then normalized to the standard space (e.g. MNI152) for group-wise comparison in voxel-based or region of interest (ROI)-based scale. Here, we followed this general pipeline with CAT12 toolbox (Farokhian et al., 2017), and projected the normalized GM maps (mapped to the 1 mm MNI152 space, with an isotropic Gaussian kernel of 8 mm for smoothing) to the AAL atlas to quantify the basal ganglia structures that were also measured by AccuBrain, including bilateral amygdala, hippocampus, thalamus, caudate, putamen and pallidum. A normalization process (regional brain volume/ICV × 100%) was also performed for the volumes of these structures as quantified by VBM.

2.4. Statistical analyses

2.4.1. Group comparison of brain regional volumetry

The volumetric differences of brain structures (quantified by AccuBrain) among CI_L, CI_R and NC groups were measured with one-way analysis of covariance (ANCOVA). Regarding the group comparisons of CI_L vs. NC and CI_R vs. NC, the covariates were age and gender. When comparing CI_L and CI_R groups, scan time interval after stroke was additionally covaried out. The multiple comparison corrections were also performed for the ANCOVA analyses, with Bonferroni correction for between-group comparisons and false discovery rate (FDR) correction for between-region comparisons. The volumetric differences were treated as significant if the corrected $p < .05$.

2.4.2. Brain volumetry-based structural covariance

As most studies that investigated structural covariance were based on the VBM pipeline, we first performed structural covariance analyses within the regions that were both quantified by VBM (through AAL atlas in the standard space) and AccuBrain (with multiple brain atlases that adapt to individual brain difference for anatomical segmentation) as aforementioned for validation. Subsequently, we further performed a structural covariance analysis with additional regions quantified by AccuBrain (basal ganglia structures: accumbens area and ventral DC; infratentorial structures: midbrain, pons, medulla and SCP) to provide a more complete map of anatomical connections within the subcortical regions for the study cohort. Here, the brain volumetric structural covariance (or anatomic connection) was defined as the correlation between the regional brain volumetric measures of different brain regions. Partial correlation analyses were performed between the volumetric measures of these regions for each group respectively.

In detail, for the CI_L vs. NC comparison, the correlations (which served as edges connecting the nodes of ROIs) were calculated between regional brain volumes of the selected ROIs in CI_L group and in NC group separately, with age and gender as the covariates for NC group, and age, gender, scan time interval after stroke and lesion size as the covariates for CI_L group. Here, only a significant correlation between two ROIs was displayed with an edge between the nodes (i.e. ROIs), and the edge was encoded with colors with respect to the magnitude of the corresponding correlation. By comparing the significant ROI-ROI correlations (volumetry-based connection) after FDR correction in different groups, we defined an ROI-ROI correlation as additional connection if it was significant in CI_L group but not in NC group. Likewise, if an ROI-ROI correlation was significant in NC group but not in CI_L group, it was defined as a missing connection in subcortical stroke patients. Here, the additional connections in CI_L group indicated the synergy volume alteration between the regions, and the missing connections in CI_L group denoted the disconnection of these regions. Regarding the CI_R vs. NC comparison, the partial correlation analyses and relevant volumetry-based connection definitions were similar. In this way, we measured the alterations of volumetric structural covariance caused by subcortical stroke and the potential lesion-side effect by comparing the alterations of volumetry-based anatomic connections in CI_L and CI_R groups.

2.4.3. Associations of brain volumetric measures with motor function after stroke

The regions that presented atrophy in CI_L (or CI_R) group

Table 1
Characteristics of the subjects.

Characteristics	NC (n = 63)	CI_L (n = 46)	CI_R (n = 33)	p-Value
Age, years	55.29 ± 7.95	54.70 ± 8.22	54.91 ± 8.60	0.930
Gender, male/female	36/27	36/10	20/13	0.063
Lesion size, ml	/	0.47 ± 1.14	0.29 ± 0.35	0.300
Scan time interval after stroke, months	/	18.96 ± 14.04	16.45 ± 10.65	0.197
ADL	/	96.08 ± 9.04	97.73 ± 7.99	0.147
Fugl_Meyer Assessment				
Upper extremity	/	58.74 ± 15.97	59.24 ± 15.58	0.633
Whole extremity	/	90.67 ± 20.13	90.79 ± 20.14	0.727

compared with NC subjects were selected to associate with FMA scores within the CI_L (or CI_R) group. The association of brain parenchyma with FMA scores were also investigated for CI_L and CI_R groups as a reference. In these analyses, age, gender, education year and lesion size were entered as covariates as they are potential confounders for motor function after stroke (Chen et al., 2000; Putman et al., 2007; Ones et al., 2009), and each time a region-specific volumetric measure was entered in a linear regression model as the independent variable on top of the covariates. The change of explained variance and the associated significance level before and after adding this regional volumetric measure was evaluated, which indicated the association of atrophy in this region with upper extremity or whole extremity.

3. Results

3.1. Demographic and clinical parameters

The characteristics of the subjects were shown in Table 1. There were no significant differences in age and gender. The scan time interval after stroke, lesion size, FMA and activities of daily living (ADL) score were similar in CI_L group and CI_R group.

3.2. Group comparison of brain regional volumetry

The group comparison of brain volumetric differences (CI_L vs. NC, CI_R vs. NC, or CI_L vs. CI_R) were shown in Table 2. There were no significant volumetric changes of brain parenchyma in CI_L group and CI_R group compared with NC group (Table 2). Regarding the regional volumetric changes in CI_L or CI_R group, the regions that presented significant atrophy generally involved internal capsule and neighboring structures (thalamus, putamen, pallidum and ventral DC) and lateral ventricle (Fig. 2) that were close to infarct location. Of note, some remote infratentorial regions also had significant atrophy in subcortical stroke patients compared with NC, such as midbrain (Fig. 2). Moreover, the side of the significant regions in comparisons of CI_L vs. NC or CI_R vs. NC largely depend on the infarct side (i.e., the regions with significant atrophy in CI_L or CI_R group compared with NC were in the ipsilesional hemisphere), and the significant regions of these two comparisons were generally symmetric. Comparing CI_L and CI_R groups, the volumetric differences mainly involved basal ganglia structures (e.g. ventral DC, thalamus, putamen and pallidum).

3.3. Brain volumetry-based structural covariance

Using the volumetric measures of 12 typical basal ganglia structures quantified by AccuBrain and VBM, the identified trends of changes in structural covariance were similar. As shown in Fig. 3, both analyses from the two tools revealed increased anatomical connections in CI_L patients compared with NC, and slightly interrupted anatomical connections in CI_R patients compared with NC. Of note, the anatomical connections identified by VBM-based method were much more extensive than those by AccuBrain, which might result from the use of single atlas (AAL) instead of multiple atlases that account for more detailed individual volumetric differences as in AccuBrain. Also, the different sensitivity of the two tools to lesion signals on T1-weighted images may also contribute to the difference of their identified structural covariances (Fig. 4). The structural covariance based on these 12 regions were also visualized in a node-edge manner (Fig. 5) for the

Table 2
Brain regions with volumetric changes.

Region	Volume ratio (% of ICV)			CI_L vs. NC	CI_R vs. NC	CI_L vs. CI_R
	NC (n = 63)	CI_L (n = 46)	CI_L (n = 33)	Corrected p	Corrected p	Corrected p
Brain parenchyma	79.157 ± 1.653	78.491 ± 1.643	78.294 ± 1.992	0.276	0.056	1.000
Lateral ventricle (L)	0.5644 ± 0.2165	0.7350 ± 0.3015	0.6941 ± 0.3065	0.013[a]	0.066	1.000
Lateral ventricle (R)	0.5261 ± 0.1913	0.6177 ± 0.2627	0.6748 ± 0.2874	0.321	0.014[a]	1.000
Hippocampus (L)	0.2467 ± 0.0188	0.2514 ± 0.0246	0.2505 ± 0.0287	1.000	1.000	1.000
Hippocampus (R)	0.2497 ± 0.0177	0.2544 ± 0.0225	0.2516 ± 0.0201	0.835	1.000	1.000
Amygdala (L)	0.1246 ± 0.0092	0.1271 ± 0.0092	0.1251 ± 0.0097	1.000	1.000	1.000
Amygdala (R)	0.1486 ± 0.0112	0.1509 ± 0.0107	0.1477 ± 0.0093	1.000	1.000	0.770
Thalamus (L)	0.4924 ± 0.0310	0.4412 ± 0.0445	0.4883 ± 0.0323	< 0.001[a]	1.000	< 0.001[a]
Thalamus (R)	0.4635 ± 0.0277	0.4607 ± 0.0370	0.4051 ± 0.0453	1.000	< 0.001[a]	< 0.001[a]
Caudate (L)	0.1982 ± 0.0200	0.2056 ± 0.0241	0.2381 ± 0.0301	0.208	1.000	0.770
Caudate (R)	0.2271 ± 0.0232	0.2322 ± 0.0205	0.3440 ± 0.0289	0.461	0.285	1.000
Putamen (L)	0.3519 ± 0.0271	0.3262 ± 0.0348	0.3440 ± 0.0289	0.004[a]	0.945	0.562
Putamen (R)	0.3376 ± 0.0265	0.3311 ± 0.0341	0.2994 ± 0.0417	1.000	< 0.001[a]	0.006[a]
Pallidum (L)	0.1010 ± 0.0087	0.0945 ± 0.0088	0.0985 ± 0.0079	0.013[a]	0.945	0.770
Pallidum (R)	0.1011 ± 0.0090	0.0998 ± 0.0095	0.0878 ± 0.0136	1.000	< 0.001[a]	< 0.001[a]
Accumbens area (L)	0.0303 ± 0.0036	0.0289 ± 0.0033	0.0305 ± 0.0044	0.333	1.000	0.770
Accumbens area (R)	0.0325 ± 0.0034	0.0316 ± 0.0037	0.0317 ± 0.0038	0.816	1.000	1.000
Ventral DC (L)	0.1464 ± 0.0103	0.1376 ± 0.0095	0.1460 ± 0.0125	< 0.001[a]	1.000	0.015[a]
Ventral DC (R)	0.1580 ± 0.0098	0.1553 ± 0.0090	0.1470 ± 0.0143	0.461	< 0.001[a]	0.025[a]
Midbrain	0.3846 ± 0.0187	0.3690 ± 0.0238	0.3704 ± 0.0244	0.013[a]	0.018[a]	1.000
Pons	0.9466 ± 0.0864	0.9139 ± 0.0729	0.9163 ± 0.0880	0.321	0.612	1.000
Medulla	0.2813 ± 0.0195	0.2683 ± 0.0160	0.2706 ± 0.0257	0.028[a]	0.186	1.000
SCP	0.0114 ± 0.0012	0.0108 ± 0.0012	0.0111 ± 0.0012	0.211	1.000	1.000

The brain volumetric measures of the three groups with p-values from ANCOVA analyses were displayed here.
SCP = Superior cerebellar peduncle. L, left; R, right.
[a] Significant after multiple comparison correction (Bonferroni correction between groups and FDR correction among regions).

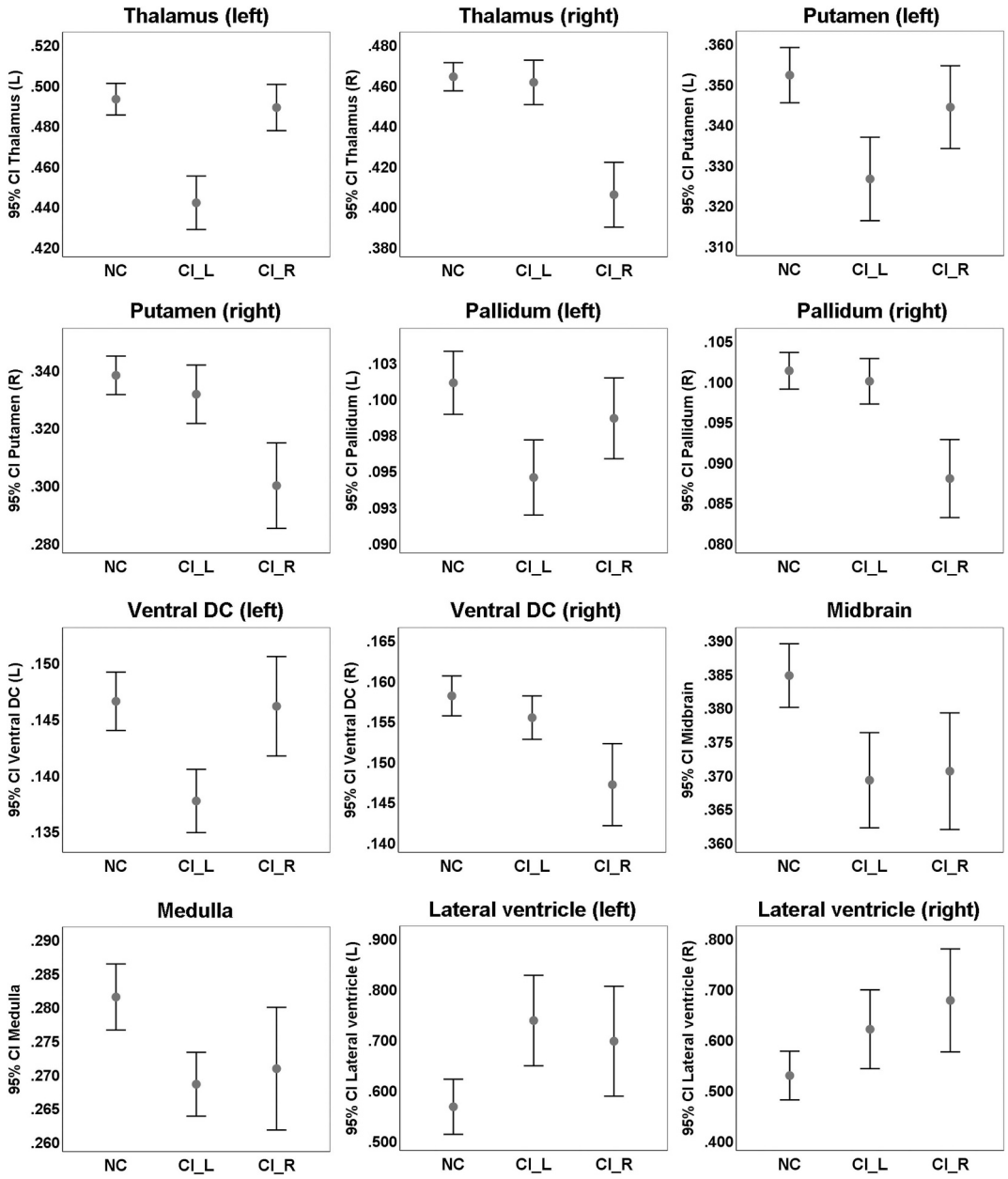

Fig. 2. Subcortical and ventricular structures with volumetric differences among the three groups. Displayed are the volume ratios of the brain regions (% of ICV). NC, normal control; CI_L, subjects with subcortical infarcts in the left hemisphere; CI_R, subjects with subcortical infarcts in the right hemisphere.

results from the volumetric measures of AccuBrain. Here, the nodes indicated the regions to be investigated, and the edges indicated the significant correlations between volumetric measures of specific regions (nodes), where the magnitude of the correlation coefficients was encoded with color from yellow to red for the edges. In CI_L and CI_R groups, the gray edges indicated missing connections (ROI-ROI correlations once significant in NC group but not in CI_L or CI_R group), and the dotted edges in yellow to red indicated additional connections (ROI-ROI correlations significant in CI_L or CI_R group but not in NC group). This node-edge graph made it easier to identify detailed differences of structural covariance between groups compared with the correlation matrix as in Fig. 4.

With the additionally quantified subcortical and infratentorial regions from AccuBrain, more extensive changes of anatomical connections were identified according to the node-edge graph (Fig. 6) with the same visualization manner as in Fig. 5. The alterations of volumetric connections (including additional and missing connections) in CI_L and CI_R patients not only involved the basal ganglia structures that were adjacent to lesioned areas, but also involved some remote structures in the infratentorial regions. In addition, in both CI_L and CI_R groups, the number of additional or missing volumetric connections were very similar in the ipsilesional hemisphere and contralesional hemisphere (Table 3). In line with the previous analyses with only basal ganglia structures, this analysis with infratentorial regions considered also revealed that the anatomical connection changes were more extensive in CI_L group than CI_R group (57 vs. 37), in terms of both additional connections and missing connections compared with NC group (Fig. 6, Table 3). Furthermore, there were more additional connections than missing connections (37 vs. 20) in CI_L group, while there were more missing connections than additional connections (25 vs. 12) in CI_R group (Table 3). The ROIs that triggered the most changes of anatomical connections included the left and right putamen in CI_L group (total change of 13 connections) and right pallidum (total change of 9 connections) in CI_R group. Of note, although all the regions that

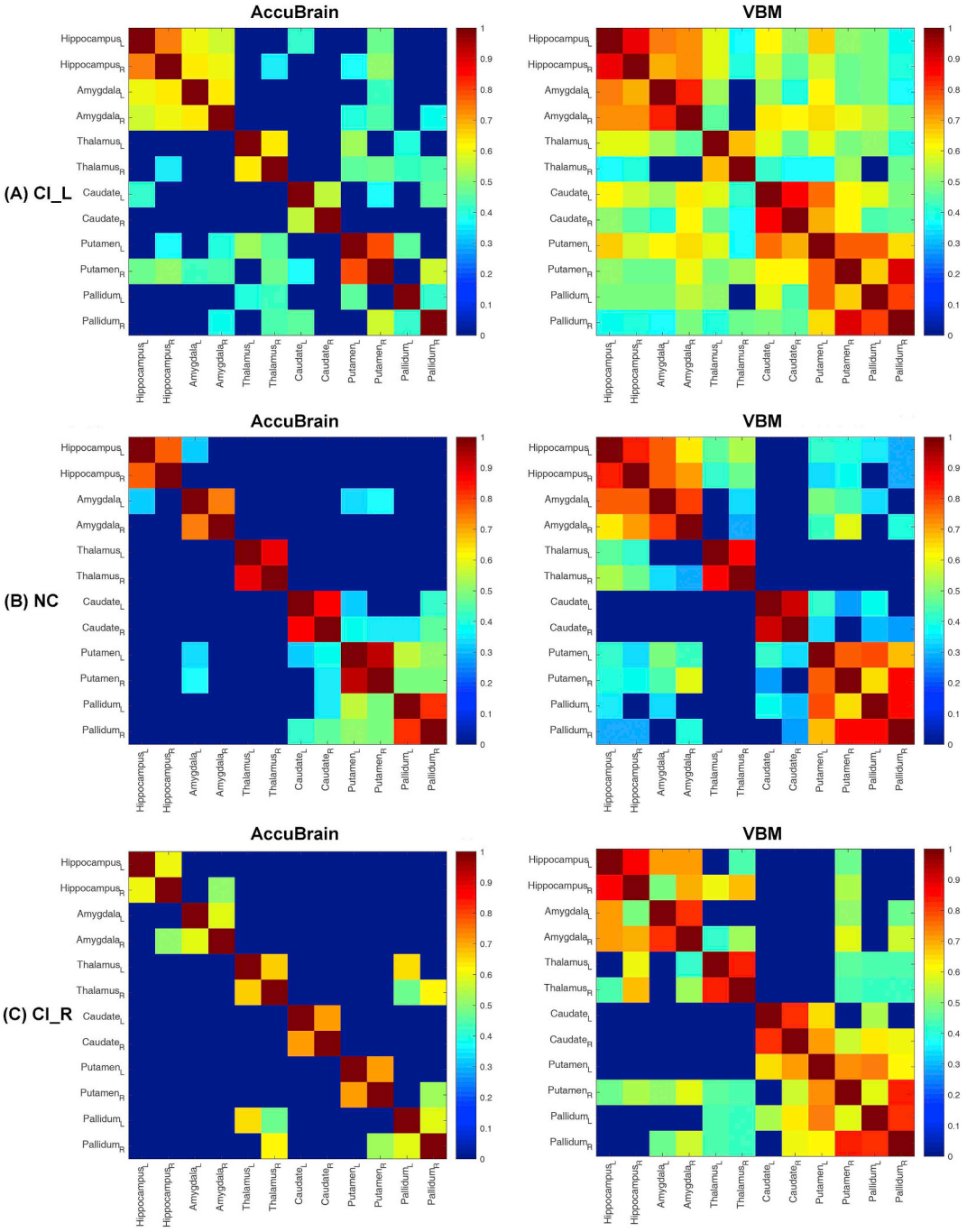

Fig. 3. The structural covariance matrix in the subcortical regions that are both quantified by AccuBrain and VBM. Bar indicates the partial correlation coefficient between ROI-specific volumetric measures. Only the significant correlations that survive FDR correction are shown; the non-significant correlations are changed to zero (dark blue in the grid panel). CI = internal capsular. L, left; R, right. (For interpretation of the references to colour in this figure legend, the reader is referred to the web version of this article.)

presented significant atrophy (in CI_L vs. NC or CI_R vs. NC comparison) triggered changes of anatomical connections in CI_L or CI_R group, they not necessarily induced more connection changes than other regions with no significant atrophy (e.g. connection changes of 4 from left thalamus vs. 9 from right pallidum in CI_L group, Table 3).

3.4. Associations of brain volumetric measures with motor function after stroke

The size of infarct was significantly associated with upper extremity and whole extremity after stroke in CI_L group but not in CI_R group (Tables 4 and 5). Among the regional volumetric measures that entered in the linear regression models as independent variables, only the volume of left lateral ventricle was significantly associated with both upper extremity and whole extremity scores of FMA ($p < .05$) in CI_L group. In contrast, most regions that presented atrophy in CI_R group (compared with NC) were associated with upper extremity and whole extremity of FMA ($p < .05$), where the volumetric measures of right thalamus presented the most significant association with FMA ($p < .001$). Furthermore, while the ROI that triggered most changes of anatomic connections in CI_L group (left putamen with a total change of 13 connections) was not associated with either score of FMA in terms of

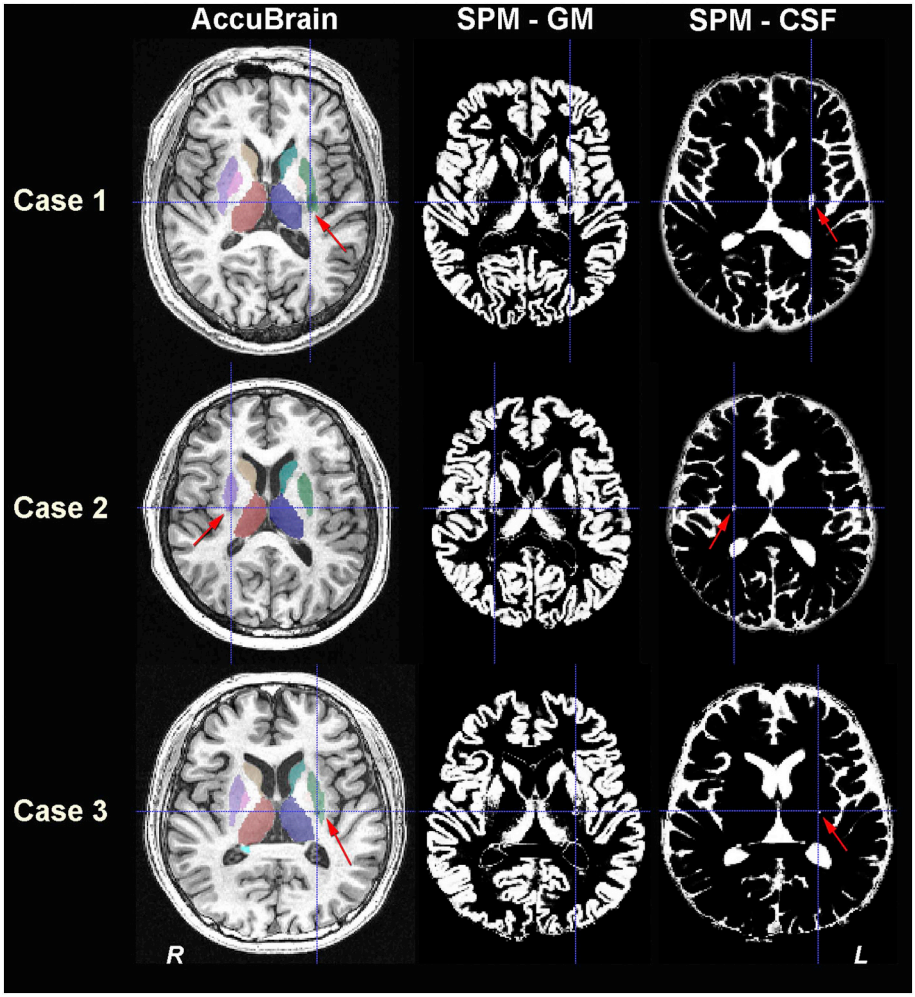

Fig. 4. Sample cases of anatomical segmentation results in individual space from AccuBrain and SPM. Three typical cases involving segmentation of lesioned regions are provided. The red arrows point to the segmentation mask that covered the lesion(s) and the blue crosshairs highlight the lesion locations. The first column displays the segmentations of basal ganglia structures from AccuBrain; the second and third column display the tissue segmentation results of gray matter (GM) and cerebrospinal fluid (CSF) from SPM. *Case 1*: a subject with a large infarct in the left basal ganglia (total lesion size = 0.76 ml). *Case 2*: a subject with infarct in the right basal ganglia (lesion size = 0.20 ml). *Case 3*: a subject with infarct in the left basal ganglia (lesion size = 0.09 ml). L, left; R, right. (For interpretation of the references to colour in this figure legend, the reader is referred to the web version of this article.)

brain volumetry (Tables 3 and 4), the ROI that triggered most connection changes in CI_R group (right pallidum with a total change of 9 connections) presented significant associations with both scores of FMA (Tables 3 and 5).

4. Discussion

In this study, we applied automated brain volumetry to measure the alterations of regional brain volumes and volumetric structural covariance after subcortical stroke, with a focus on subcortical regions. Chronic stroke patients with CI infarct showed extensive brain atrophy relative to healthy controls, involving not only the subcortical regions of infarction lesion, but also remote regions (such as midbrain). In addition, the side of these influenced regions largely depended on the side of the infarct. Moreover, this study identified the significant changes of structural covariance in subcortical stroke patients using brain volumetry from automatic anatomical segmentations. Also, the lesion-side effect of anatomical reorganization was also found in subcortical stroke patients.

Among the identified brain regions with volumetric loss in stroke patients, many were the lesioned regions with infarction, including putamen, pallidum, thalamus and ventral DC. The ischemic infarct may influence the blood supply in lesioned regions and thus caused brain tissue loss in these regions. In addition, we found enlarged unilateral ventricle at the side of the infarct in stroke patients, which may result from brain tissue loss in the lesioned subcortical regions that are adjacent to ventricle. Furthermore, we found volumetric loss in the remote regions (midbrain, medulla oblongata) that involved the motor pathway in subcortical stroke patients. As we all know, the corticospinal tract connects the internal capsule region (with stroke lesion in this study) and the cerebral peduncle at the base of the midbrain, and this tract passes through brainstem from pons to medulla. Accordingly, the volumetric loss of the infratentorial regions may result from the Wallerian degeneration of the distal parts in the nervous systems following the injury of proximal axon or cell body (Yu et al., 2009). These results were in line with previous studies that reported the structural damage in remote regions in subcortical stroke, which was caused by axonal degeneration secondary to the occurrence of stroke lesions (Diao et al., 2017a,b). However, volumetric alterations of infratentorial regions were rarely reported in patients with subcortical stroke. The secondary brain structural atrophy may be the underlying cause of stroke-induced behavioral deficits (Delavaran et al., 2017) in the chronic stage, although the relevant mechanism needs to be further validated in future studies. Finally, these significantly altered regions were generally symmetric for CI_L and CI_R groups depending on the side of the infarct (i.e. regions with significant volumetric changes were in the ipsilesional hemisphere), suggesting that different neural substrates may underlie structural impairment. Thus, the lesion-side effect should be considered in future studies on stroke patients.

For the first time, we applied automated brain volumetry to measure the structural covariance (or volumetric anatomical connection) in subcortical stroke patients. In a sub-analysis of the 12 basal ganglia structures in comparison with VBM-based method, the two methods identified similar pattern of structural covariance changes in subcortical stroke patients, where there were more additional anatomical connections in CI_L group than CI_R group and more missing

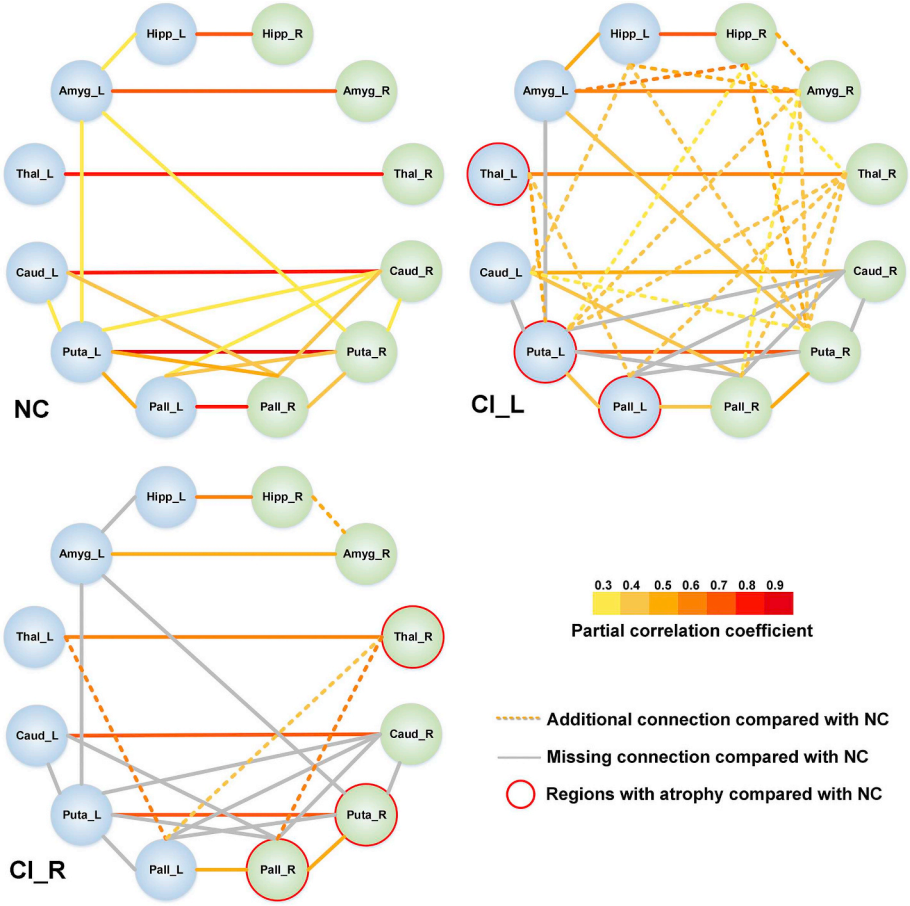

Fig. 5. Structural covariance of the predefined subcortical structures (12 regions) in normal controls and subcortical stroke patients with CI infarct in the left or right hemisphere. The nodes indicate the volumetric measures of specific regions of interest (ROIs), where the structures in the left hemisphere are colored blue and the structures in the right hemisphere are colored in green. The edges in yellow to red indicate the significant volumetric connections ($p < .05$ with FDR correction) measured by partial correlation coefficients between the regional volumes of ROIs, where the color indicates the value of a partial correlation. The dotted lines (edges) indicate the additional connection in CI_L or CI_R group compared with NC group, and the gray lines (edges) indicate the missing connection in CI_L or CI_R group compared with NC group. The regions with significant atrophy in CI_L or CI_R compared with NC are marked with red circle.
CI = internal capsular; Hipp = hippocampus; Amyg = amygdala; Caud = caudate; Puta = putamen; Pall = pallidum. L, left; R, right. (For interpretation of the references to colour in this figure legend, the reader is referred to the web version of this article.)

connections in CI_R group than CI_L group (Fig. 3). Of note, the anatomic connections found in VBM-based method were more extensive that those identified with automated brain volumetry from AccuBrain. As we did not repair the misclassification of tissues in VBM-based method (see Fig. 4 for three typical cases, where lesion signals were treated as CSF), this misclassification might contribute to the difference of structural covariance. However, compared with the previous studies where the repairment of lesion misclassification was performed (Fan et al., 2013; Abela et al., 2015), the lesion size in our subcortical stroke cohort was much smaller (median lesion volume of 0.16 ml in our cohort vs. > 3.48 ml (Abela et al., 2015) and 7.70 ml (Fan et al., 2013) in previous studies), and was only 10% of the volume of the smallest basal ganglia structure (i.e. pallidum, with a median volume of 1.57 ml for left pallidum and 1.58 ml for right pallidum in NC group). This indicated that the misclassification of lesion could not result in such big difference of structural covariance results in the two methods, and there should be other reasons that contributed much more than the misclassification issue. It should be noted that previous studies have demonstrated the poor agreement of VBM-based quantification of subcortical structures with manual segmentation results compared with anatomical segmentation tools (Naess-Schmidt et al., 2016), which might induce further difference in structural covariance based on brain volumetry. In this regard, multi-atlas-based segmentation tool such as AccuBrain would be recommended for quantification of brain volumetry and the subsequent volumetric structural covariance analysis in the future.

When some subcortical and infratentorial regions were additionally considered, the patterns of structural covariance changes were generally similar but with more extensive network-level reorganizations (Fig. 6). Compared with normal controls, infarcts in the CI_L and CI_R groups not only involved additional connections in the basal ganglia structures that were adjacent to lesioned areas, but also involved alterations of some connections in remote areas (brainstem structures). These results might indicate the same or synergy volume alteration between the regions, where the involved alterations in remote regions have been proposed to corroborate with the concept of structural connectional diaschisis (Carrera and Tononi, 2014; Veldsman, 2017). In addition, the extensive alterations of structural covariance in CI_L and CI_R not only involved the regions that presented atrophy compared with NC, but also the regions that presented no significant volumetric difference with NC. In fact, both the ipsilesional hemisphere and the contralesional hemisphere were involved in the changes of anatomic connections, and the changes between ipsilesional and contralesional hemispheres were relatively symmetric. This indicated that the reorganization of anatomic connections during the chronic phase of subcortical stroke was in a whole-brain network level, independent of lesion side and location of regional atrophy.

Within the extensive change of structural covariance within the subcortical structures, we found that lateral putamen (total change of 13 connections) and right pallidum (total change of 9 connections) were most intensively involved in the alterations of anatomic connections for CI_L group and CI_R group respectively (Table 3 and Fig. 6). Previous studies reported that the thalamus (which was adjacent to putamen and pallidum) seemed to be vulnerable to degeneration after stroke and might serve as a multi-network hub that involves vast functional interconnectedness (Stebbins et al., 2008; Hwang et al., 2017). Although the thalamus was not the most involved in alterations of structural covariance in our study, it may contribute to the alterations of anatomic connections of its adjacent regions such as pallidum and putamen. In this regard, our structural covariance results corroborated with the previous finding and further revealed the involvement of the adjacent regions to thalamus in a network level of volumetric

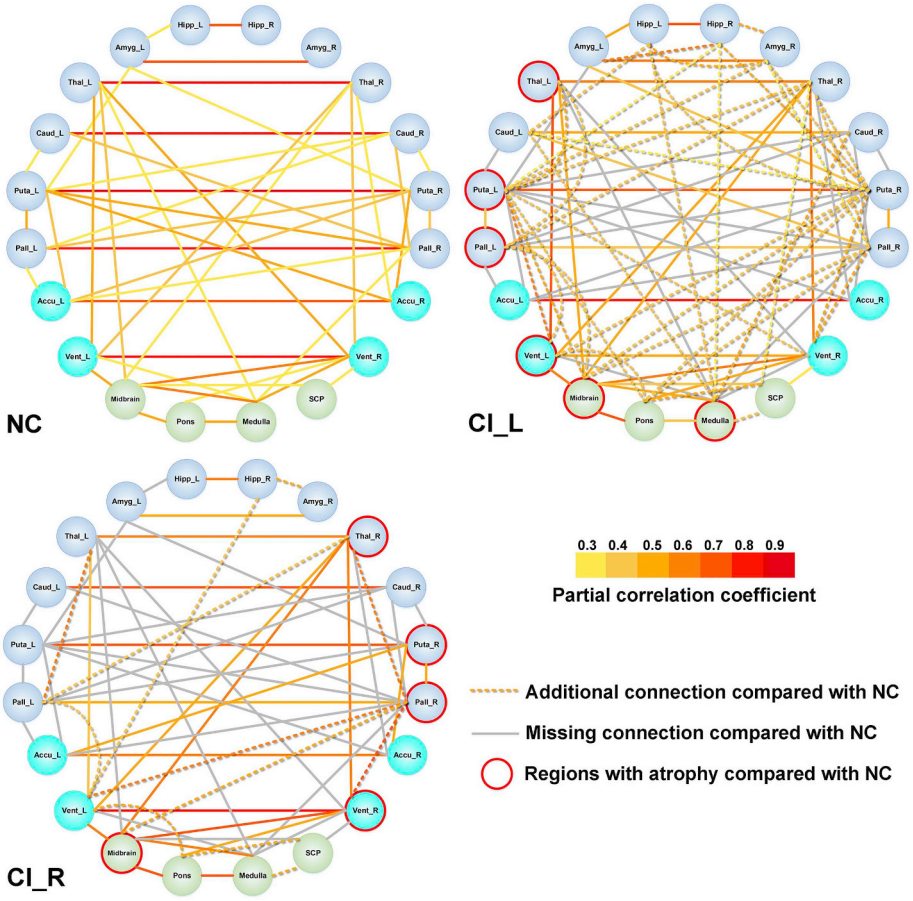

Fig. 6. Volumetric structural covariance in patients with left/right CI infarct and normal controls using automated brain volumetry from AccuBrain (20 regions). The nodes indicate the volumetric measures of specific regions of interest (ROIs), where the basal ganglia structures both quantified by AccuBrain and SPM are colored with dark blue, the basal ganglia structures only quantified by AccuBrain are colored in light blue, and the brainstem structures specifically quantified AccuBrain are colored in green. The edges in yellow to red indicate the significant volumetric connections ($p < .05$ with FDR correction) measured by partial correlation coefficients between the regional volumes of ROIs, where the color indicates the value of a partial correlation. The dotted lines (edges) indicate the additional connection in CI_L or CI_R group compared with NC group, and the gray lines (edges) indicate the missing connection in CI_L or CI_R group compared with NC group. The regions with significant atrophy in CI_L or CI_R compared with NC are marked with red circle.
CI = internal capsular; Hipp = hippocampus; Amyg = amygdala; Caud = caudate; Puta = putamen; Pall = pallidum; Accu = Accumbens area; Vent = Ventral DC; SCP = Superior cerebellar peduncle. L, left; R, right. (For interpretation of the references to colour in this figure legend, the reader is referred to the web version of this article.)

Table 3
Difference of volumetry-based anatomical connection in subjects with CI infarct compared with NC.

Node ROI	Subjects with CI_L infarct			Subjects with CI_R infarct		
	Missing connection	Additional connection	Total change[b]	Missing connection	Additional connection	Total change[b]
Hippocampus L	0	4	4	1	0	1
Hippocampus R	0	5	5	0	2	2
Amygdala L	1	1	2	3	0	3
Amygdala R	0	4	4	0	1	1
Thalamus L	2	2	4[a]	3	1	4
Thalamus R	1	5	6	1	2	3[a]
Caudate L	1	3	4	2	0	2
Caudate R	4	1	5	4	0	4
Putamen L	6	7	13[a]	7	0	7
Putamen R	4	9	13	3	0	3[a]
Pallidum L	3	4	7[a]	4	3	7
Pallidum R	4	5	9	5	4	9[a]
Accumbens area L	4	0	4	3	0	3
Accumbens area R	3	0	3	2	0	2
Ventral DC L	1	4	5[a]	1	4	5
Ventral DC R	2	3	5	3	1	4[a]
Midbrain	0	4	4[a]	2	1	3[a]
Pons	0	5	5	0	2	2
Medulla	4	5	9[a]	4	1	5
SCP	0	3	3	2	2	4
Left hemisphere	9	12.5	21.5	12	4	16
Right hemisphere	9	16	25	9	5	14
Total	**20**	**37**	**57**	**25**	**12**	**37**

SCP = Superior cerebellar peduncle. L, left; R, right.
[a] Regions with significant volumetric differences in CI_L or CI_R group compared with NC group (Table 2).
[b] The sum of missing and additional connections compared in CI_L/CI_R group compared with NC group.

Table 4
Associations of brain volumetric measures with motor function in CI_L patients.

Model	Independent variable	FMA (upper)			FMA (whole)		
		R square	*p*-Value	Beta (SE)	R square	*p*-Value	Beta (SE)
1	Age, gender, education	0.041	0.709	–	0.061	0.550	–
1a	Model 1 + Lesion size[a]	0.356	< 0.001	−52.253 (13.200)	0.343	< 0.001	−62.648 (16.906)
2	Model 1a + Scan time interval[c]	0.360	0.652	0.067 (0.147)	0.348	0.633	0.091 (0.188)
3a	Model 2 + Brain parenchyma	0.362	0.776	0.407 (1.416)	0.354	0.605	0.944 (1.807)
3b	Model 2 + Lateral ventricle L	0.493	0.009[b]	−23.925 (8.523)	0.499	0.005[b]	−32.285 (10.751)
3c	Model 2 + Thalamus L	0.361	0.825	−13.986 (62.762)	0.348	0.979	2.127 (80.415)
3d	Model 2 + Putamen L	0.363	0.732	25.904 (74.900)	0.353	0.618	48.270 (95.675)
3e	Model 2 + Pallidum L	0.417	0.099	473.902 (277.961)	0.410	0.086	628.754 (354.572)
3f	Model 2 + Ventral DC L	0.361	0.891	41.199 (297.287)	0.350	0.736	129.308 (379.981)
3 g	Model 2 + Midbrain	0.365	0.639	−47.101 (99.310)	0.352	0.684	−52.222 (127.257)
3 h	Model 2 + Medulla	0.407	0.136	−250.948 (163.760)	0.408	0.091	−361.803 (207.435)

The results of stepwise linear regression are displayed here. R square is the explained variance in corresponding behavior score. The p-value indicates the difference in explained variance (R square) between the model (e.g. Model 3a) and the previous model (Model 2). Unstandardized coefficients (beta) with SE (standard error) are provided.

[a] The lesion size was normalized by individual intracranial volume in the same way as the regional brain volumes (% of ICV).

[b] The regional brain atrophy measure that has significant impact on upper extremity or whole extremity on top of age, gender, education level, lesion size and scan time interval after stroke.

[c] Scanning time after stroke in months.

Table 5
Associations of brain volumetric measures with motor function in CI_R patients.

Model	Independent variable	FMA (upper)			FMA (limbs)		
		R square	*p*-Value	Beta (SE)	R square	*p*-Value	Beta (SE)
1	Age, gender, education	0.056	0.662	–	0.045	0.739	–
1a	Model 1 + Lesion size[a]	0.062	0.691	−5.302 (13.180)	0.048	0.767	−5.146 (17.154)
2	Model 1a + Scan time interval[c]	0.066	0.761	0.097 (0.316)	0.052	0.744	0.136 (0.411)
3a	Model 2 + Brain parenchyma	0.079	0.554	1.206 (2.009)	0.063	0.607	1.365 (2.619)
3b	Model 2 + Lateral ventricle R	0.204	0.052	−23.570 (11.518)	0.187	0.058	−29.973 (15.045)
3c	Model 2 + Thalamus R	0.412	0.001[b]	292.139 (77.637)	0.412	0.001[b]	384.682 (100.291)
3d	Model 2 + Putamen R	0.208	0.049[b]	233.172 (112.252)	0.179	0.067	283.889 (147.677)
3e	Model 2 + Pallidum R	0.258	0.020[b]	689.535 (276.674)	0.245	0.021[b]	892.679 (360.450)
3f	Model 2 + Ventral DC R	0.250	0.023[b]	581.623 (239.620)	0.240	0.023[b]	758.653 (311.582)
3 g	Model 2 + Midbrain	0.254	0.021[b]	307.918 (124.947)	0.232	0.026[b]	388.730 (163.770)

The results of stepwise linear regression are displayed here. R square is the explained variance in corresponding behavior score. The p-value indicates the difference in explained variance (R square) between the model (e.g. Model 3a) and the previous model (Model 2). Unstandardized coefficients (beta) with SE (standard error) are provided.

[a] The lesion size was normalized by individual intracranial volume in the same way as the regional brain volumes (% of ICV).

[b] The regional brain atrophy measure that has significant impact on upper extremity or whole extremity on top of age, gender, education level and lesion size.

[c] Scanning time after stroke in months.

changes after subcortical stroke.

Moreover, we identified the lesion-side effect of the alterations of structural covariance in subcortical stroke patients. In general, the right-handed subcortical stroke patients with lesions in the left hemisphere showed more extensive changes in volumetric structural covariance than those with lesions in the right hemisphere compared with healthy controls. In addition, the ratio of additional anatomical connections to missing connections was inverse in CI_L and CI_R groups, with more additional connections in CI_L groups and more missing connections in CI_R group. A previous study reported the right-sided stroke patients presented different cortical gray matter changes compared with left-sided ones (Diao et al., 2017a,b), which also revealed a lesion-side effect, although they did not involve the volumetric changes of subcortical structures. This may also ascribe to the fact that right-handed patients with a left-dominant hemisphere stroke have less ability on daily life basis than those with lesions in the right hemisphere, which leading to faster degeneration of these regions in CI_L patients, as well as, the synergy volume alteration between the regions were more significant.

Finally, we evaluated the influence of atrophy of different brain regions on motor function for CI_L and CI_R groups respectively. While no regions with atrophy were associated with either score of FMA in CI_L group, almost all the structures that presented atrophy in CI_R group were associated with both scores of FMA. In addition, the region that triggered most anatomical connection changes in CI_L (i.e. left putamen) was not associated with motor function, but the one for CI_R group (i.e. right pallidum) was significantly associated with motor function (Tables 4 and 5). In fact, these results corroborated with the lesion-side effect identified in our structural covariance analyses, as the broader reorganization of volumetric structural covariance in CI_L group than CI_R group may influence the association between the volumetric measure of a single region and the motor function after stroke, even if this region was located in the motor pathway.

There were also some limitations of this study. First, the durations between stroke onset and MRI scanning in the study cohort were quite variable, ranging from 6 to 70 months. This might mix the results of different stages post-stroke and thus influence the specify and generalizability of our findings, although we have covaried out the duration after stroke onset in the analyses. Second, the longitudinal changes of brain volumetry and volumetric connection following subcortical stroke, which are of larger clinical interest as they would help to highlight the dynamic process of brain volume changes, cannot be

investigated with our cross-sectional study design. Also, a longitudinal design making subjects as their own controls will reduce the inter-individual variability in the measurements. In addition, as stroke may induce an ischemic cascade that initiates or aggravates neurodegenerative processes that lead to brain atrophy, it is possible that some regional differences between groups could have been observed before stroke events (i.e. patients prone to have subcortical stroke symptoms may have a reduced brain volume). Therefore, longitudinal studies are essential to separate the effects of ischemic infarct from accelerated atrophy occurring on the background of long-term vascular risk factors and mixed pathologies (Veldsman, 2017). Finally, the brain volumetric covariance analysis was a zero time-lagged correlation to measure the synchronization, therefore, it cannot allow quantification of the possible causal relationships between the significant brain regions. In the future, longitudinal studies should be performed to investigate the dynamic brain volumetric changes and causal relationships of structural alterations among brain regions after subcortical stroke.

In conclusion, this study identified the brain volumetric changes and the alterations of structural covariance in chronic subcortical stroke patients. These alterations involved lesioned areas as well as remote areas to infarct location, which reflects the potential impact of subcortical infarct on brain structural impairments. In addition, these results revealed the different anatomical connections patterns in patients with subcortical stroke largely depend on lesion-side, highlighting the importance of the individualized research on the structural underpinnings of brain dysfunction after stroke in the future study.

Acknowledgement

We are indebted to our patients and their caregivers for generously supporting our study. This study was supported by the Natural Science Foundation of China (Nos. 81601467, 81601472, 81871327).

Conflict of interest statement

L.S. is the director of BrainNow Medical Technology Limited, the company that owns the image analysis software *AccuBrain®* that is used in this study. L.Z. and Y.L. are now employed by BrainNow Medical Technology Limited. All other authors report no financial relationships with commercial interests.

References

Abela, E., Missimer, J.H., Federspiel, A., Seiler, A., Hess, C.W., Sturzenegger, M., et al., 2015. A thalamic-fronto-parietal structural covariance network emerging in the course of recovery from hand paresis after ischemic stroke. Front. Neurol. 6, 211.

Abrigo, J., Shi, L., Luo, Y., Chen, Q., Chu, W.C.W., Mok, V.C.T., et al., 2018. Standardization of hippocampus volumetry using automated brain structure volumetry tool for an initial Alzheimer's disease imaging biomarker. Acta Radiol. https://doi.org/10.1177/0284185118795327. (Epub ahead of print).

Alexander-Bloch, A., Giedd, J.N., Bullmore, E., 2013a. Imaging structural co-variance between human brain regions. Nat. Rev. Neurosci. 14 (5), 322–336.

Alexander-Bloch, A., Raznahan, A., Bullmore, E., Giedd, J., 2013b. The convergence of maturational change and structural covariance in human cortical networks. J. Neurosci. 33 (7), 2889–2899.

Anderson, B.J., Eckburg, P.B., Relucio, K.I., 2002. Alterations in the thickness of motor cortical subregions after motor-skill learning and exercise. Learn. Mem. 9 (1), 1–9.

Benjamin, P., Lawrence, A.J., Lambert, C., Patel, B., Chung, A.W., MacKinnon, A.D., et al., 2014. Strategic lacunes and their relationship to cognitive impairment in cerebral small vessel disease. Neuroimage Clin 4, 828–837.

Bernhardt, B.C., Worsley, K.J., Besson, P., Concha, L., Lerch, J.P., Evans, A.C., et al., 2008. Mapping limbic network organization in temporal lobe epilepsy using morphometric correlations: insights on the relation between mesiotemporal connectivity and cortical atrophy. NeuroImage 42 (2), 515–524.

Carrera, E., Tononi, G., 2014. Diaschisis: past, present, future. Brain 137 (9), 2408–2422 (Pt.

Cauda, F., Nani, A., Costa, T., Palermo, S., Tatu, K., Manuello, J., et al., 2018. The morphometric co-atrophy networking of schizophrenia, autistic and obsessive spectrum disorders. Hum. Brain Mapp. 39 (5), 1898–1928.

Chen, C.L., Tang, F.T., Chen, H.C., Chung, C.Y., Wong, M.K., 2000. Brain lesion size and location: effects on motor recovery and functional outcome in stroke patients. Arch. Phys. Med. Rehabil. 81 (4), 447–452.

Chiu, H.C., Damasio, A.R., 1980. Human cerebral asymmetries evaluated by computed tomography. J. Neurol. Neurosurg. Psychiatry 43 (10), 873–878.

Chong, C.D., Dumkrieger, G.M., Schwedt, T.J., 2017. Structural co-variance patterns in migraine: a cross-sectional study exploring the role of the hippocampus. Headache 57 (10), 1522–1531.

Corballis, M.C., 2014. Left brain, right brain: facts and fantasies. PLoS Biol. 12 (1), e1001767.

Delavaran, H., Jonsson, A.C., Lovkvist, H., Iwarsson, S., Elmstahl, S., Norrving, B., et al., 2017. Cognitive function in stroke survivors: a 10-year follow-up study. Acta Neurol. Scand. 136 (3), 187–194.

Diao, Q., Liu, J., Wang, C., Cao, C., Guo, J., Han, T., et al., 2017a. Gray matter volume changes in chronic subcortical stroke: a cross-sectional study. Neuroimage Clin 14, 679–684.

Diao, Q., Liu, J., Wang, C., Cheng, J., Han, T., Zhang, X., 2017b. Regional structural impairments outside lesions are associated with verbal short-term memory deficits in chronic subcortical stroke. Oncotarget 8 (19), 30900–30907.

DuPre, E., Spreng, R.N., 2017. Structural covariance networks across the life span, from 6 to 94 years of age. Netw Neurosci 1 (3), 302–323.

Fan, F., Zhu, C., Chen, H., Qin, W., Ji, X., Wang, L., et al., 2013. Dynamic brain structural changes after left hemisphere subcortical stroke. Hum. Brain Mapp. 34 (8), 1872–1881.

Farokhian, F., Beheshti, I., Sone, D., Matsuda, H., 2017. Comparing CAT12 and VBM8 for detecting brain morphological abnormalities in temporal lobe epilepsy. Front. Neurol. 8, 428.

Fazekas, F., Chawluk, J.B., Alavi, A., Hurtig, H.I., Zimmerman, R.A., 1987. MR signal abnormalities at 1.5 T in Alzheimer's dementia and normal aging. AJR Am. J. Roentgenol. 149 (2), 351–356.

Hafkemeijer, A., Altmann-Schneider, I., de Craen, A.J., Slagboom, P.E., van der Grond, J., Rombouts, S.A., 2014. Associations between age and gray matter volume in anatomical brain networks in middle-aged to older adults. Aging Cell 13 (6), 1068–1074.

Hwang, K., Bertolero, M.A., Liu, W.B., D'Esposito, M., 2017. The human thalamus is an integrative hub for functional brain networks. J. Neurosci. 37 (23), 5594–5607.

Jiang, Y., Luo, C., Li, X., Duan, M., He, H., Chen, X., et al., 2018. progressive reduction in gray matter in patients with schizophrenia assessed with MR imaging by using causal network analysis. Radiology 287 (2), 633–642.

Kim, H., Kim, J., Loggia, M.L., Cahalan, C., Garcia, R.G., Vangel, M.G., et al., 2015. Fibromyalgia is characterized by altered frontal and cerebellar structural covariance brain networks. Neuroimage Clin 7, 667–677.

Lee, P.L., Chou, K.H., Lu, C.H., Chen, H.L., Tsai, N.W., Hsu, A.L., et al., 2018. Extraction of large-scale structural covariance networks from grey matter volume for Parkinson's disease classification. Eur. Radiol. 28 (8), 3296–3305.

LeMay, M., 1986. Left-right temporal region asymmetry in infants and children. AJNR Am. J. Neuroradiol. 7 (5), 974.

Liu, F., Zhuo, C., Yu, C., 2016. Altered cerebral blood flow covariance network in schizophrenia. Front. Neurosci. 10, 308.

Liu, F., Tian, H., Li, J., Li, S., Zhuo, C., 2018. Altered voxel-wise gray matter structural brain networks in schizophrenia: association with brain genetic expression pattern. Brain Imaging Behav. https://doi.org/10.1007/s11682-018-9880-6. (Epub ahead of print).

Mechelli, A., Friston, K.J., Frackowiak, R.S., Price, C.J., 2005. Structural covariance in the human cortex. J. Neurosci. 25 (36), 8303–8310.

Naess-Schmidt, E., Tietze, A., Blicher, J.U., Petersen, M., Mikkelsen, I.K., Coupe, P., et al., 2016. Automatic thalamus and hippocampus segmentation from MP2RAGE: comparison of publicly available methods and implications for DTI quantification. Int. J. Comput. Assist. Radiol. Surg. 11 (11), 1979–1991.

Nestor, S.M., Gibson, E., Gao, F.Q., Kiss, A., Black, S.E., Alzheimer's Disease Neuroimaging, I., 2013. A direct morphometric comparison of five labeling protocols for multi-atlas driven automatic segmentation of the hippocampus in Alzheimer's disease. NeuroImage 66, 50–70.

Nestor, S.M., Misic, B., Ramirez, J., Zhao, J., Graham, S.J., Verhoeff, N., et al., 2017. Small vessel disease is linked to disrupted structural network covariance in Alzheimer's disease. Alzheimers Dement. 13 (7), 749–760.

Ones, K., Yalcinkaya, E.Y., Toklu, B.C., Caglar, N., 2009. Effects of age, gender, and cognitive, functional and motor status on functional outcomes of stroke rehabilitation. NeuroRehabilitation 25 (4), 241–249.

Putman, K., De Wit, L., Schoonacker, M., Baert, I., Beyens, H., Brinkmann, N., et al., 2007. Effect of socioeconomic status on functional and motor recovery after stroke: a European multicentre study. J. Neurol. Neurosurg. Psychiatry 78 (6), 593–599.

Sanabria-Diaz, G., Melie-Garcia, L., Iturria-Medina, Y., Aleman-Gomez, Y., Hernandez-Gonzalez, G., Valdes-Urrutia, L., et al., 2010. Surface area and cortical thickness descriptors reveal different attributes of the structural human brain networks. NeuroImage 50 (4), 1497–1510.

Seeley, W.W., Crawford, R.K., Zhou, J., Miller, B.L., Greicius, M.D., 2009. Neurodegenerative diseases target large-scale human brain networks. Neuron 62 (1), 42–52.

Stebbins, G.T., Nyenhuis, D.L., Wang, C., Cox, J.L., Freels, S., Bangen, K., et al., 2008. Gray matter atrophy in patients with ischemic stroke with cognitive impairment. Stroke 39 (3), 785–793.

Veldsman, M., 2017. Brain atrophy estimated from structural magnetic resonance imaging as a marker of large-scale network-based neurodegeneration in aging and stroke. Geriatrics 2 (4), 34.
Wang, C., Qin, W., Zhang, J., Tian, T., Li, Y., Meng, L., et al., 2014. Altered functional organization within and between resting-state networks in chronic subcortical infarction. J. Cereb. Blood Flow Metab. 34 (4), 597–605.
Whitwell, J.L., Crum, W.R., Watt, H.C., Fox, N.C., 2001. Normalization of cerebral volumes by use of intracranial volume: implications for longitudinal quantitative MR imaging. Am. J. Neuroradiol. 22 (8), 1483–1489.
Yu, C., Zhu, C., Zhang, Y., Chen, H., Qin, W., Wang, M., et al., 2009. A longitudinal diffusion tensor imaging study on Wallerian degeneration of corticospinal tract after motor pathway stroke. NeuroImage 47 (2), 451–458.
Zhang, J., Meng, L., Qin, W., Liu, N., Shi, F.D., Yu, C., 2014. Structural damage and functional reorganization in ipsilesional m1 in well-recovered patients with subcortical stroke. Stroke 45 (3), 788–793.